

Probing Local Structural Events in β -Hairpin Unfolding with Transient Nonlinear Infrared Spectroscopy**

Adam W. Smith and Andrei Tokmakoff*

Contemporary descriptions of protein-folding pathways have been greatly enhanced by the study of single-domain peptides.^[1,2] Hairpins in particular have been used to investigate the role of β turns in secondary-structure stability and have also been used to explore the stabilizing effect of tertiary side-chain contacts.^[2–5] Transient folding studies are particularly valuable because β hairpins are frequently used to compare and test theoretical protein-folding models.^[2,6–8] To date, however, fast folding experiments on the nanosecond to microsecond timescale are limited in their level of structural detail. Previous hairpin-folding studies have probed either the transient fluorescence of side-chain chromophores^[9,10] or the transient infrared absorbance of the amide I band,^[11,12] a congested spectral feature consisting of delocalized CO vibrations of the peptide backbone.^[13,14] Here we report on an experimental method that increases the structural resolution of amide I' spectroscopy to probe the unfolding kinetics of individual amino acid residues on a submicrosecond timescale following a temperature jump (T jump).

A combination of two methods is used to elucidate detailed structural information from T -jump amide I vibrational spectroscopy. First, $^{13}\text{C}'$ isotope labeling is used to spectrally isolate individual amino acid residues within the hairpin sequence. Amide I' spectral features are separated and assigned with two-dimensional infrared (2D IR) spectroscopy. Second, dispersed vibrational echo (DVE) spectroscopy is used to probe the sample following a T jump of approximately 10°C within a nanosecond. The primary advantage of the nonlinear IR techniques over traditional absorbance experiments is that they are sensitive to vibrational couplings and different line-broadening mechanisms. In this report, these methods are used to study the turn region and cross-strand contacts of the de novo peptide, PG12.^[3] The V3-E4 amide group, which is involved in cross-strand hydrogen bonding, is found to unfold on a timescale of 130 ns. Furthermore, it is found that the turn region of PG12 does *not* undergo significant structural change during the T jump. These experimental observations are consistent with unfold-

ing of the peptide by fraying at the N and C termini. The results represent an important step toward building an experimentally verified hairpin-folding mechanism.

The hairpin-folding mechanisms that have been proposed are guided by two principle paradigms. The first is the kinetic zipper model, in which formation of the β turn is the important nucleation event that triggers the zipping together of cross-strand contacts beginning at the turn and continuing to the termini.^[15] In the second model, folding begins with the collapse of the hydrophobic side-chain groups, following which the backbone contacts return to their native state.^[16] Deviations from these two models have been observed in simulation studies, where the folding mechanisms are distinguished by more subtle structural events. Some of these events include partial hydrophobic collapse, fraying of the N- and C-terminal residues, the ordering of the cross-strand hydrogen bonds, the formation of salt bridges between cross-strand side chains, and rearrangements of the hydrophobic core.^[6,8,17–19] The timescale and relative importance of these events has been discussed in a number of publications, but experimental data has not been able to directly distinguish between the proposed models.

While no decisive method has been developed, kinetic experiments have provided considerable insight. Side-chain fluorescence studies can resolve structural changes within the hydrophobic core. Such measurements assign folding times ranging from 5–10 μs ,^[9,11,20] although in some systems, this rate has been seen to vary depending on starting conditions.^[10] Amide I transient absorbance methods have been carried out for a number of hairpin peptides. Typical timescales are on the order of 10 μs ,^[12,21,22] although faster kinetics have been observed in cyclic peptides^[23] or in peptides with a proline-enhanced β turn.^[22,24,25] In addition, mutation studies have been combined with spectroscopic probes to investigate the role of specific residues on the folding rate.^[21] The key information that is unavailable in any of these studies is the folding rate of individual backbone contacts—particularly the hydrogen-bond contacts that help stabilize the β -sheet secondary structure.

Isotope-edited amide I spectroscopy is one route towards obtaining site-specific information on polypeptides.^[26] When a ^{13}C atom is substituted at the C' position, the amide I vibrational frequency is reduced by approximately 40 cm^{-1} , which isolates it from the main amide I' band. The frequency shift effectively decouples the oscillator from the other vibrations so that it is approximately 90% localized on the labeled amide group.^[14] This effect has been used to investigate the amide I band of β -hairpin peptides^[14,27,28] and has also been used to study various other peptides and proteins.^[26,29,30] Here the technique is used to spectrally isolate

[*] A. W. Smith, Prof. A. Tokmakoff
Department of Chemistry
Massachusetts Institute of Technology
77 Massachusetts Avenue, Cambridge, MA 02139 (USA)
Fax: (+1) 617-253-7372
E-mail: tokmakoff@mit.edu
Homepage: <http://web.mit.edu/tokmakofflab/>

[**] This work was supported by a grant from the National Science Foundation (CHE-0616575).

Supporting information for this article is available on the WWW under <http://www.angewandte.org> or from the author.

two peptide groups on PG12, a 12-residue hairpin with a D-proline-enhanced type II' β turn.^[3]

The FTIR spectrum of unlabeled PG12 (PG12-UL) has three amide I peaks (Figure 1). The most intense peak (ν_{\perp})

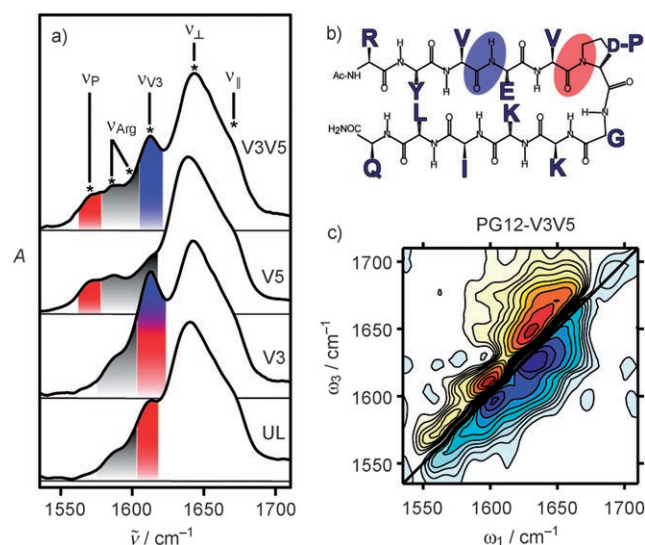


Figure 1. a) The FTIR absorbance spectrum is shown for each PG12 isotopologue. The positions of the ν_p and ν_{v3} peaks are highlighted in red and blue, respectively. Each spectrum was recorded in pH 3.8 deuterated acetate buffer. b) The sequence of PG12 is highlighted with colored circles to show the position of the labeled amide groups. c) Absorptive 2D IR spectrum is shown for PG12-V3V5 with contours at $\pm 3, 6, 9, 12, 16, 24, 32, 45, 65$, and 85% .

corresponds to a delocalized vibration in which the amide groups oscillate in phase across the strand and out of phase with their nearest neighbor.^[14] The shoulder region near 1674 cm^{-1} (ν_{\parallel}) is a more complicated set of vibrations that often involve the amide groups oscillating in phase with their nearest neighbor and out of phase across the strand.^[14] The peak at 1613 cm^{-1} (ν_p) is localized on the Val-Pro amide group.^[14] It is red-shifted from the main amide I band because the proline N_{α} forms a tertiary amide, whereas the other peptide groups are secondary amides.^[31]

As can be seen in Figure 1, a single $^{13}\text{C}'$ substitution at the Val5 position (PG12-V5) shifts the ν_p peak to 1561 cm^{-1} (42 cm^{-1}). The same isotopic substitution at the Val3 position (PG12-V3) brings one of the main amide transitions (ν_{v3}) out to 1612 cm^{-1} . In PG12 V3, ν_{v3} lies on top of the ν_p peak, but in the doubly labeled species there is an approximately 40-cm^{-1} separation between the ν_p and ν_{v3} vibrations, and between the ν_{v3} and ν_{\perp} vibrations. These distinct spectral markers allow the transient folding experiment to simultaneously and independently probe the kinetics of the turn and midstrand region of the peptide. Finally, we note that a comparison of all FTIR spectra indicates that each also contains two additional weak peaks at 1590 cm^{-1} and 1610 cm^{-1} . These are assigned to the symmetric and asymmetric CN stretches of the protonated arginine side chain.^[32]

These amide I spectral features are more clearly observed with 2D IR spectroscopy. We use a femtosecond Fourier transform method to obtain an absorptive spectrum that

correlates the frequency of vibrational excitation (ω_1) with a detection frequency (ω_3).^[33] The spectrum for PG12-V3V5 is shown in Figure 1, and others are given in the Supporting Information. There are several key pieces of information available in a 2D IR spectrum. First, cross peaks in a 2D IR spectrum directly report on the coupling between amide vibrations and help to diminish problems with spectral congestion. This has been particularly valuable in detecting and understanding the ν_{\perp} and ν_{\parallel} modes of β -sheet proteins and peptides.^[34] The cross peak between the two modes (observed as a ridge along $\omega_3 = \omega_1$) has been observed in a number of proteins^[35] and was used to identify cross-strand contacts in a β hairpin at high temperatures.^[36] In addition to these features, the 2D IR spectrum of PG12-V3V5 shows two distinct features on the diagonal corresponding to the V3- and V5-labeled peptide groups in the linear spectrum. The cross peak between ν_p and $\nu_{\perp}/\nu_{\parallel}$ is weak, indicating that the label effectively decouples the peptide unit from the other amide vibrations. Cross peaks are visible in the spectral regions connecting the ν_{v3} and $\nu_{\perp}/\nu_{\parallel}$ peaks, indicating coupling between those modes. Additionally, the 2D line shape independently reports on the inhomogeneous (diagonal) and homogeneous (antidiagonal) contributions to the linewidth.^[33] This information can be used to characterize structural heterogeneity, which is always ambiguous in a one-dimensional absorbance spectrum. Temperature-dependent 2D IR spectra found in the Supporting Information reveal a linear increase in homogeneous linewidth with temperature, for both labeled and unlabeled peaks.

DVE spectroscopy is a one-dimensional variant of 2D IR spectroscopy that is measured by probing the sample with three time-coincident femtosecond infrared pulses and spectrally dispersing the emitted nonlinear signal field.^[37] DVE spectroscopy has the advantage of being much easier to perform and is background free. The DVE spectrum is equivalent to the projection of the absolute value of the complex 2D IR spectrum onto the ω_3 axis,^[37] making it possible to use the 2D IR spectrum to interpret the features of a DVE spectrum taken under identical conditions (see the Supporting Information). For example, off-diagonal intensity in the 2D IR spectrum contributes to the diagonal peak intensity to sharpen the features of the DVE spectrum relative to the FTIR spectrum. Interference between the positive and negative peaks of the 2D IR spectrum lead to shifted peak positions in the DVE spectrum relative to the measured frequencies in the 2D IR and FTIR spectra. This is most striking in the ν_B , ν_{v3} , and ν_{\perp} peaks of PG12-V3V5 (Figure 2), which are red-shifted nearly 10 cm^{-1} relative to the FTIR spectrum.

Changes to the DVE spectrum with temperature can best be explained in terms of the corresponding changes in the 2D IR spectrum, given in the Supporting Information. First, any increase in the homogeneous or inhomogeneous line width will lead to a lower DVE signal because anti-diagonal and diagonal line widths project equally onto the ω_3 axis. The second cause of lower DVE signal is a loss in coupling seen as decreased cross peak intensity in the 2DIR spectrum. A third contribution to lower DVE peaks is a decrease in diagonal peak intensity, which is caused by temperature-dependant

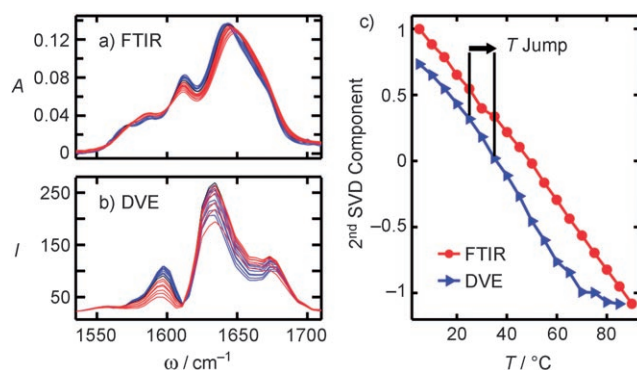


Figure 2. a) Amide I FTIR spectra of PG12-V3V5 from 5 to 90°C. The spectra are colored blue from 5 to 40°C, black at 45°C, and red from 50 to 95°C. The frequency axis is the same for plots (a) and (b). b) DVE spectra of PG12-V3V5 from 5 to 85°C. The coloring scheme is the same in (a) except the red spectra which range from 50 to 85°C. c) Melting curves calculated using the FTIR and DVE spectra from 1540 to 1710 cm^{-1} . The melting curves are plotted as the value of the second component at each temperature. The DVE curve is offset from the FTIR data by -0.25 for clarity.

changes to the vibrational eigenstates that that report on the disordering of the peptide.

The equilibrium DVE spectra of PG12 and PG12-V3V5 are shown in Figure 2 for temperatures from 15 to 45°C. Spectral changes are shown with the second-component spectrum of a singular value decomposition. As the temperature is raised, the intensity of the ν_{\parallel} and ν_{\perp} peaks increases. Over this temperature range we assign the change to increasing amide I intensity corresponding to disordered peptide ($\approx 1650 \text{ cm}^{-1}$) and the increased transmission of the excitation and signal pulses due to the temperature-dependent solvent absorbance. At 50°C (see Figure 2 and the Supporting Information) the ν_{\parallel} and ν_{\perp} peaks begin to decrease with increasing temperature, indicating that the contributions from the increasing disorder and linewidths are overcoming the solvent transmittance effects. The ν_{P} peak in both PG12 and PG12-V3V5 exhibits very little change, which we interpret as reflecting negligible structural changes in that part of the peptide. The ν_{Arg} and ν_{V3} peaks decrease as the temperature is raised, which is attributed to an increase in structural disorder.

Transient thermal unfolding of PG12 and PG12-V3V5 was probed by recording the entire amide I DVE spectrum at time delays (τ) following a T jump of 10°C. Changes to the DVE signal of PG12-V3V5 from 10 ns to 1 μs are shown in Figure 3 for four frequency windows. Transient data was also acquired to delays times of $\tau = 50 \text{ ms}$ and was observed to relax with the 2-ms temperature re-equilibration of the sample. The transient solvent response is plotted in black as a reference for the temperature profile. The ν_{\perp} , ν_{\parallel} , and ν_{P} frequency regions each have rise times of 10 ns, which is on the same order as the 8-ns instrument response time. This timescale reflects spectral changes that track the increased solvent temperature. In addition, the ν_{\perp} peak displays a small (2%) decrease that has a fitted decay time of 610 ns. This decay time corresponds generally to thermally induced disorder within the peptide. Changes to the ν_{P} peak are small in magnitude which leads us

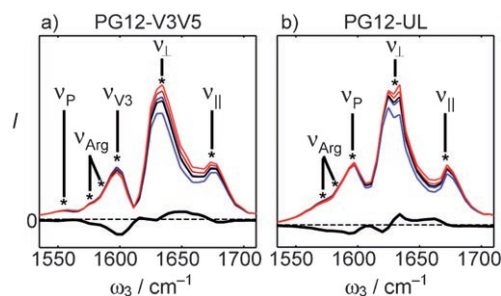


Figure 3. Equilibrium DVE spectra of PG12 (a) and PG12-V3V5 (b) from 15°C (blue) to 45°C (red). The solid black plots are the second SVD component spectra calculated over the same temperature range. As the temperature is raised, the intensity at ν_{\perp} and ν_{\parallel} increases, while the ν_{P} , ν_{SC} , and ν_{V3} intensity decreases.

to conclude that the Val5-Pro6 amide group does not undergo significant structural changes during the T jump of 10°C. This conclusion is corroborated by the ν_{P} transient of PG12-UL (see the Supporting Information) and the temperature-dependant intensity profile of the peak in the equilibrium DVE data which is plotted explicitly in the Supporting Information.

Changes to the ν_{V3} peak in PG12-V3V5 are much slower than the 10-ns rise time of the other spectral features. The exponential fit shown in Figure 3 has a time constant of $(135 \pm 50) \text{ ns}$, and the magnitude and sign of the transient difference signal match the equilibrium spectra. Structurally, the change is indicative of increased disorder at the Val3-Glu4 amide group. Because the amide frequency is closely correlated with hydrogen-bonding strength, this timescale probes disordering of the cross-strand hydrogen-bond contacts (Figure 4).

The observed transient DVE signal of the ν_{V3} and ν_{P} peaks puts detailed structural constraints on proposed unfolding models for this system. Specifically, the results support an

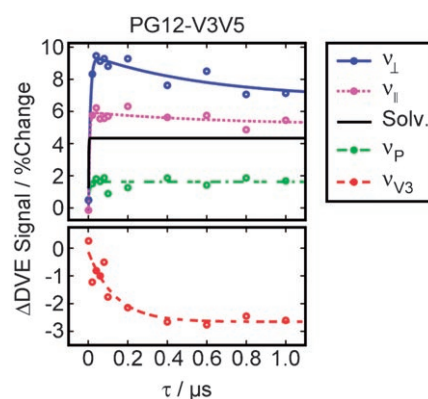


Figure 4. Transient DVE signal of PG12-V3V5 at four frequency channels. Each data point is the average of over the following frequency ranges: 1558–1567 cm^{-1} (red), 1598–1607 cm^{-1} (green), 1639–1648 cm^{-1} (violet), 1668–1678 cm^{-1} (blue). The fitted transient absorbance of the solvent is scaled by 150 and plotted in black. Open circles correspond to measured data, and the lines are single exponential fits to the data. The τ_1 rise time of the fits to the ν_{\perp} , ν_{\parallel} , and ν_{P} data is less than 10 ns, and the fitted τ_1 decay time of the ν_{V3} peak is $135 \pm 50 \text{ ns}$. The ν_{\perp} and ν_{\parallel} signals each have subsequent decay times of 610 and 680 ns, respectively.

unfolding model for this peptide in which the turn region does not undergo significant structural variation and the midstrand region is disrupted on a 130-ns timescale. This timescale is about five times faster than the slow decay of the ν_{\perp} peak (610 ns) and suggests that the mid strand region denatures before the rest of the peptide. The unfolding time of the midstrand region is one to two orders of magnitude faster than the observed folding time of many other β hairpins. However, it is similar to the unfolding times of cyclic hairpins^[23] as well as that of a three-stranded β -sheet peptide containing D-Pro enhanced β turns.^[24] It is therefore possible that the T jump transients describe the sampling of an increased configurational space about the folded structure at the elevated temperature rather than a full unfolding trajectory.^[38] This would also be consistent with the finding that tightly folded hairpins such as PG12 and TrpZip2 have a highly heterogeneous unfolding free energy surface.^[10]

The isotope labeling approach used in this study is generally applicable to other peptides and small proteins. By incorporating isotope labels into various structural regions of a given polypeptide it is possible to study a mechanism on the residue level. Nonlinear IR probes like 2D IR and DVE spectroscopy are uniquely sensitive to vibrational coupling and line shapes. The spectral signatures, which report on structural disorder and tertiary contacts, such as hydrogen bonding across β strands, explore essential physical events during thermally induced peptide unfolding. Such studies will significantly accelerate our understanding of peptide and protein folding.

Received: March 16, 2007

Revised: June 11, 2007

Published online: September 13, 2007

Keywords: IR spectroscopy · isotope labeling · peptides

- [1] J. Kubelka, J. Hofrichter, W. A. Eaton, *Curr. Opin. Struct. Biol.* **2004**, *14*, 76–88.
- [2] M. S. Searle, B. Ciani, *Curr. Opin. Struct. Biol.* **2004**, *14*, 458–464.
- [3] H. E. Stanger, S. H. Gellman, *J. Am. Chem. Soc.* **1998**, *120*, 4236–4237.
- [4] J. F. Espinosa, F. A. Syud, S. H. Gellman, *Protein Sci.* **2002**, *11*, 1492–1505.
- [5] A. G. Cochran, N. J. Skelton, M. A. Starovasnik, *Proc. Natl. Acad. Sci. USA* **2001**, *99*, 9081–9081.
- [6] P. G. Bolhuis, *Biophys. J.* **2004**, *88*, 50–61.
- [7] D. K. Klimov, D. Thirumalai, *Proc. Natl. Acad. Sci. USA* **2000**, *97*, 2544–2549.
- [8] W. Y. Yang, J. W. Pitera, W. C. Swope, M. Gruebele, *J. Mol. Biol.* **2004**, *336*, 241–251.
- [9] V. Muñoz, P. A. Thompson, J. Hofrichter, W. A. Eaton, *Nature* **1997**, *390*, 196–199.
- [10] W. Y. Yang, M. Gruebele, *J. Am. Chem. Soc.* **2004**, *126*, 7758–7759.
- [11] C. D. Snow, L. Qiu, D. Du, F. Gai, S. J. Hagen, V. S. Pande, *Proc. Natl. Acad. Sci. USA* **2004**, *101*, 4077–4082.
- [12] R. B. Dyer, S. J. Maness, E. S. Peterson, S. Franzen, R. M. Fesinmeyer, N. H. Andersen, *Biochemistry* **2004**, *43*, 11560–11566.
- [13] P. Hamm, M. Lim, R. M. Hochstrasser, *J. Phys. Chem. B* **1998**, *102*, 6123–6138.
- [14] A. W. Smith, A. Tokmakoff, *J. Chem. Phys.* **2007**, *126*, 045109–045111.
- [15] V. Munoz, E. R. Henry, J. Hofrichter, W. A. Eaton, *Proc. Natl. Acad. Sci. USA* **1998**, *95*, 5872–5879.
- [16] A. R. Dinner, T. Lazaridis, M. Karplus, *Proc. Natl. Acad. Sci. USA* **1999**, *96*, 9068–9073.
- [17] J. Tsai, M. Levitt, *Biophys. Chem.* **2002**, *101*, 187–201.
- [18] G. H. Wei, N. Mousseau, P. Derreumaux, *Proteins Struct. Funct. Genet.* **2004**, *56*, 464–474.
- [19] J. W. Pitera, I. Haque, W. C. Swope, *J. Chem. Phys.* **2006**, *124*, 141102.
- [20] V. Munoz, R. Ghirlando, F. J. Blanco, G. S. Jas, J. Hofrichter, W. A. Eaton, *Biochemistry* **2006**, *45*, 7023–7035.
- [21] D. Du, M. J. Tucker, F. Gai, *Biochemistry* **2006**, *45*, 2668–2678.
- [22] D. Du, Y. Zhu, C.-Y. Huang, F. Gai, *Proc. Natl. Acad. Sci. USA* **2004**, *101*, 15915–15920.
- [23] S. J. Maness, S. Franzen, A. C. Gibbs, T. P. Causgrove, R. B. Dyer, *Biophys. J.* **2003**, *84*, 3874–3882.
- [24] Y. Xu, P. Purkayastha, F. Gai, *J. Am. Chem. Soc.* **2006**, *128*, 15836–15842.
- [25] Y. Xu, R. Oyola, F. Gai, *J. Am. Chem. Soc.* **2003**, *125*, 15388–15394.
- [26] S. M. Decatur, *Acc. Chem. Res.* **2006**, *39*, 169–175.
- [27] V. Setnicka, R. Huang, C. L. Thomas, M. A. Etienne, J. Kubelka, R. P. Hammer, T. A. Keiderling, *J. Am. Chem. Soc.* **2005**, *127*, 4992–4993.
- [28] J. P. Wang, J. X. Chen, R. M. Hochstrasser, *J. Phys. Chem. B* **2006**, *110*, 7545–7555.
- [29] S. H. Brewer, B. Song, D. P. Raleigh, R. B. Dyer, *Biochemistry* **2007**, *46*, 3279–3285.
- [30] J. H. Werner, R. B. Dyer, R. M. Fesinmeyer, N. H. Andersen, *J. Phys. Chem. B* **2002**, *106*, 487–494.
- [31] J. Hilario, J. Kubelka, T. A. Keiderling, *J. Am. Chem. Soc.* **2003**, *125*, 7562–7574.
- [32] Y. N. Chirgadze, O. V. Fedorov, N. P. Trushina, *Biopolymers* **1975**, *14*, 679.
- [33] M. Khalil, N. Demirdöven, A. Tokmakoff, *J. Phys. Chem. A* **2003**, *107*, 5258–5279.
- [34] C. M. Cheatum, A. Tokmakoff, J. Knoester, *J. Chem. Phys.* **2004**, *120*, 8201–8215.
- [35] N. Demirdöven, C. M. Cheatum, H. S. Chung, M. Khalil, J. Knoester, A. Tokmakoff, *J. Am. Chem. Soc.* **2004**, *126*, 7981–7990.
- [36] A. W. Smith, H. S. Chung, Z. Ganim, A. Tokmakoff, *J. Phys. Chem. B* **2005**, *109*, 17025–17027.
- [37] H. S. Chung, M. Khalil, A. W. Smith, Z. Ganim, A. Tokmakoff, *Proc. Natl. Acad. Sci. USA* **2005**, *102*, 612–617.
- [38] B. Zagrovic, C. D. Snow, S. Khaliq, M. R. Shirts, V. S. Pande, *J. Mol. Biol.* **2002**, *323*, 153–164.